J. Hydrol. Hydromech., 67, 2019, 4, 359–371
DOI: 10.2478/johh-2019-0015

Extension of the Gardner exponential equation to represent the hydraulic conductivity curve

Theophilo B. Ottoni Filho[1], Marlon G. Lopes Alvarez[2], Marta V. Ottoni[3*], Arthur Bernardo Barbosa Dib Amorim[1]

[1] Department of Water Resources and Environment, Politechnical School, Federal Univ. of Rio de Janeiro (CT/UFRJ), Ilha do Fundão, Rio de Janeiro, RJ, Brazil. CEP: 21941-909
[2] State Environmental Institute (INEA), Av. Venezuela 110, Saúde, Rio de Janeiro, RJ, Brazil. CEP: 20081-312.
[3] Department of Hydrology, Geological Survey of Brazil (CPRM), Av. Pasteur, 404, Urca, Rio de Janeiro, RJ, Brazil. CEP: 22290-240
[*] Corresponding author. Tel.: +55 21 2546 0352. E-mail: marta.ottoni@cprm.gov.br

Abstract: The relative hydraulic conductivity curve $K_r(h) = K/K_s$ is a key variable in soil modeling. This study proposes a model to represent $K_r(h)$, the so-called Gardner dual (GD) model, which extends the classical Gardner exponential model to h values greater than h_o, the suction value at the inflection point of the $K_r(h)$ curve in the log-log scale. The goodness of fit of GD using experimental data from UNSODA was compared to that of the MVG [two-parameter (K_{ro}, L) Mualem-van Genuchten] model and a corresponding modified MVG model (MVGm). In 77 soils without evidence of macropore flow, GD reduced the RMSE errors by 64% (0.525 to 0.191) and 29% (0.269 to 0.193) in relation to MVG and MVGm, respectively. In the remaining 76 soils, GD generally was less accurate than MVG and MVGm, since most of these soils presented evidence of macropore flow (dual permeability). GD has three parameters and two degrees of freedom, like MVG. Two of them allow the calculation of the macroscopic capillary length, a parameter from the infiltration literature. The three parameters are highly dependent on the $K_r(h)$ data measurement in a short wet suction range around h_o, which is an experimental advantage.

Keywords: Hydraulic conductivity curve; Gardner exponential model; Mualem-van Genuchten model.

INTRODUCTION

The unsaturated hydraulic conductivity curve is a key soil hydrodynamic function in water and solute transfer in the vadose zone. Variations in the $K(h)$ curve are highly non-linear with suction h ($h > 0$) at the same time that they may reach values of various orders of magnitude. This requires a reliable mathematical model of representation of this curve for the proper description of hydraulic flows. In this study, we will assume the saturated hydraulic conductivity (K_s) to be a pre-established parameter and therefore it is sufficient to consider the relative hydraulic conductivity $K_r = K/K_s$.

Thus, the choice of a mathematical model to represent the K_r vs. h data is crucial (in this study we will not use the $K_r(\theta)$ models, where θ is the volumetric water content; the suction is expressed in cm). The $K_r(h)$ curve is usually given graphically in the log-log scale (Figure 1), where log = $\log_{10}$. Figure 1 shows a typical graph with the log K_r vs. log h data plot tending to the origin (h tending to 1.0 cm and K_r tending to 1.0) in a convex curve asymptotic to the horizontal axis log h. Above certain h_o suction values, there is a general tendency to an inflection of the experimental plot and to its curvature to become concave or quasi-linear (as in Figures 2 and 3 in Peters and Durner (2008), for example). Other graphs like this one will be shown along the study. According to Peters and Durner (2008) this inflection might be caused by film flow effects which would be relevant to define $K_r(h)$ in higher suction ranges ($h > h_o$), but irrelevant and largely dominated by capillary bundle flow effects in wetter moisture ranges ($h < h_o$). Various strictly empirical equations were proposed to represent K_r vs. h data between the 1950s and 1970s, as reported by Raats and Gardner (1971), Vereecken et al. (1990) and Leij et al. (1997). The most

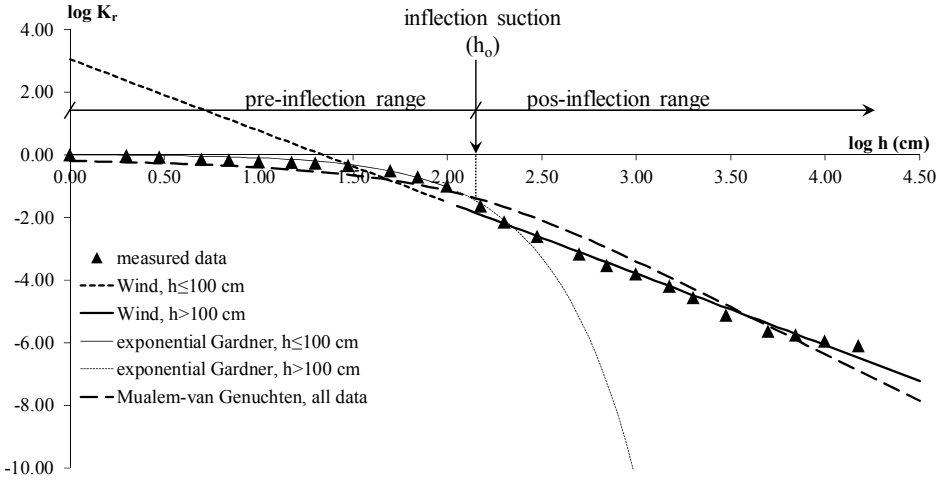

Fig. 1. Typical example [soil 4670 from the UNSODA database (Leij et al., 1996)] of representation of data of the relative conductivity curve $K_r = K/K_s$; a curve inflection tendency can be observed around suction h_o. The Wind and Gardner exponential equations were adjusted only for the measured data set with $h \geq 100$ cm or $h \leq 100$ cm, respectively. The Mualem-van Genuchten equation was adjusted for the complete data set.

commonly used, according to Vereecken et al. (1990), are those where suction appears in a power or exponential function, as shown below.

One of the pioneer and frequently used empirical equations is the Wind power equation (Wind, 1955), also called the Brooks and Corey (Leij et al., 1997) hydraulic conductivity equation, or the Campbell (Wösten et al., 2001) equation.

$$K_r = ah^{-b}, \qquad a \text{ and } b > 0. \tag{1}$$

This equation fits the log K_r vs. log h data to a straight line. It is valid only for suction values greater than a minimum value (Campbell (1974) and Poulsen et al. (1999) propose minimal values of 100 cm and 20 cm, respectively). Therefore, the model is inadequate to fit the $K_r(h)$ curve at suction ranges close to saturation, as shown in Figure 1. Outside the convex range of the data plot, some soils tend to linearity, as shown in Figure 1, which justifies using Equation (1). As the Wind equation does not apply to low suction values, it is not recommended to describe ponding or low tension infiltration flows.

The most used empirical $K_r(h)$ equation in the literature on infiltration is the Gardner one-parameter exponential model (Gardner, 1958):

$$K_r = e^{-h/\lambda}. \tag{2}$$

Parameter $\lambda > 0$, called the macroscopic capillary length (White and Sully, 1987), is expressed in cm in this paper. The sorptive number, $\alpha = 1/\lambda$ (White and Sully, 1987), is often used instead of λ. An acknowledged inconvenience of this equation is that it fits the K_r vs. h data properly generally only in a limited suction range close to saturation (Communar and Friedman, 2014; Gardner, 1958; Jarvis and Messing, 1995; Russo, 1988), as shown in the example in Figure 1, where it is inappropriate for h >100 cm, in contrast to that observed for the Wind equation. Figure 1 makes it clear that the convex part of the experimental data plot is well represented by the Gardner exponential model. Beyond inflection point h_o = 130 cm, the model results are greatly different from the experimental data.

Equation (2) is largely used because it allows linearizing the Richards equation in cases of steady (Wooding, 1968) and unsteady flows (Philip, 1969; Warrick, 1974). Based on this linearization, various analytical solutions related to infiltration have been developed for both surface and sub-surface water application methods. These solutions underlie many infiltration test methods for in-field determination of saturated hydraulic conductivity and macroscopic capillary length. The most popular tests use the steady flow condition and their most popular devices are: the ring infiltrometers (Reynolds, 2008a; Reynolds and Elrick, 1990), disk (or tension) infiltrometers (Clothier and Scotter, 2002; Reynolds, 2008b), and constant head well permeameters (Reynolds et al., 1985; Reynolds, 2008c). Analytical solutions based on Equation (2) for transient infiltration flows with various water application devices are also common in the literature (Philip, 1986; Reynolds, 2011; Vandervaere, 2002, among others), including solutions related to drip irrigation engineering (Communar and Friedman, 2014). Inversion of the Richards equation for infiltration flows using numerical methods to determine K_s and λ is also made easy by the use of Equation (2), because in this case the $K(h)$ curve requires only these two parameters, which is advantageous since the corresponding numerical scheme usually provides a single solution with efficiency and convergence (Lazarovitch et al., 2007). The great acceptability of Equation (2) to handle infiltration flows results from its generally good representation of K_r vs. h data at low suction ranges, which are the suction ranges most representative of usual infiltration processes. Another advantage of Equation (2) is that its shape parameter (λ) is a strictly hydraulic-structural soil variable, such as the saturated hydraulic conductivity (K_s), because, according to the infiltration theory by disk infiltrometers at zero suction on the imbibition surface (Vandervaere, 2002; White and Sully, 1987):

$$\lambda K_s = S_p^2 0.55/(\theta_s - \theta_i), \tag{3}$$

where θ_s and θ_i are the volumetric water content at saturation and at initial conditions before wetting, respectively, and S_p is the soil sorptivity, defined as

$$S_p = \lim_{t \to 0} \mathrm{d}I/\mathrm{d}\sqrt{t}, \tag{4}$$

where I is the cumulative infiltration (infiltration volume divided by the disk area) and t is the infiltration time. Soil sorptivity (at zero suction on the imbibition surface) depends on θ_s minus θ_i and is a measure of the capacity of the soil to absorb infiltration water strictly due to soil pressure gradients (capillarity).

The last strictly empirical equation we refer to is the Gardner power equation (Gardner, 1958):

$$K_r = (1 + ch^d)^{-1}, \qquad c \text{ and } d > 0. \tag{5}$$

As demonstrated in Figure 3 from Raats and Gardner (1971), in a log-log graph and at low suction values, Equation (5) expresses $K_r(h)$ as a convex curve asymptotic to the horizontal axis (h) and which tends to a straight line with the increase in h, that is, Equation (5) simultaneously incorporates the qualities of the Wind and Gardner exponential equations (Figure 1). In principle, this must reflect on a better fit of Equation (5) in relation to the fit of the other two equations for wider suction ranges, from saturation to high tensions. This superiority of Equation (5) was demonstrated by Vereecken et al. (1990) using a database with 45 soils. The Mualem-van Genuchten (MVG) model will be discussed next. However, in a log-log scale, similarly to the Gardner power model, it also gives a convex curve at low suctions and fits to a straight line at higher tensions (Figure 1; Figure 2 in van Genuchten, 1980). In fact, the literature confirms that at wide suction ranges Equation (5) in general has experimental data fit errors comparable to those of the MVG model (Schaap and Leij, 1998; Vereecken et al., 2010; Weynants et al., 2009).

Instead of strictly empirical relations, another tendency is to determine the $K_r(h)$ curve from the water retention curve, $\theta(h)$, as its data are more easily obtained than those of the former. For this reason, hydraulic models are recurrent in the literature dedicated to the determination of K_r based on the calculation of the porous space distribution. The abovementioned MVG model is one of such models, where:

$$K_r = S^L \left[1 - \left(1 - S^{n/(n-1)}\right)^{1-1/n}\right]^2, \tag{6}$$

$$S = S(h) = \left[1 + (\alpha h)^n\right]^{-(1-1/n)}, \tag{7}$$

$$S = \frac{\theta(h) - \theta_r}{\theta_s - \theta_r}. \tag{8}$$

Equation 6 represents the Mualem (1976) hydraulic conductivity model which can be applied to the van Genuchten expression, Equation (7) (van Genuchten, 1980), which in turn allows using suction h to calculate the soil effective saturation, S,

defined in Equation (8). In fact, Equations (7) and (8) model the water retention curve. In the MVG model, parameters θ_s (saturated water content), θ_r (residual water content), and the two shape parameters, α (cm^{-1}) and n (dimensionless), can be considered water retention curve data fitting parameters, while parameter L (pore connectivity, dimensionless) can be considered a hydraulic conductivity curve data fitting parameter (Vereecken et al., 2010). The four water retention curve parameters are positive, except θ_r, which can also be null (rarely has it been fitted with a negative value, according to Vereecken et al., 2010), and $n > 1$. Parameter L can be positive, null or negative (Schaap and Leij, 2000). MVG (Equations 6–8) is the most popular hydraulic conductivity model based on the water retention curve, among the various equivalent models that have been proposed (Kosugi et al., 2002; Leij et al., 1997). It also is the most used representation of the $K_r(h)$ curve in the mathematical simulation of flows and transport in the vadose zone (Vereecken et al., 2010). The MVG model was conceived to fit $K_r(h)$ in a wide suction range, generally from saturation to the "wilting point" [$\theta(h = 15000$ cm)]. Its most used version is the one which does not require any K_r vs. h experimental data. In this case, the default value of $L = 0.5$ is used (Mualem, 1976; van Genuchten, 1980) and the $K_r(h)$ curve can be obtained simply from the parameterization of the $\theta(h)$ curve. However, the default $L = 0.5$ must be considered cautiously, since in the study by Schaap and Leij (2000) of 235 soils from the UNSODA database (Leij et al., 1996), $L = -1$ resulted in a decrease in the mean fitting error of $K_r(h)$ by 43% (1.31 for $L = 0.5$ to 0.75 for $L = -1$).

The flexibilization of the MVG model considers a multiplicative factor ($K_{ro} \leq 1$) in Equation (6):

$$K_r = K_{ro} S^L \left[1 - \left(1 - S^{n/(n-1)}\right)^{1-1/n}\right]^2 . \quad (9)$$

This new parameterization of the MVG model (Equations (7–9)) requires two fitting parameters for the $K_r(h)$ curve, K_{ro} and L, which makes the MVG model more accurate (Veerecken et al., 2010). In fact, in the study by Schaap and Leij (2000), parameterization of Equations (7–9) applied to the authors' database led to a significant decrease in the fitting mean error of $Kr(h)$, 69%, (1.31 for $L = 0.5$, $K_{ro} = 1$, in contrast to 0.41 for flexible L and K_{ro}), in relation to the most common parameterization with default $L = 0.5$. As the focus of our study is the accuracy of the mathematical representation of the hydraulic conductivity curve in the soil moisture range from saturation to the "wilting point", the MVG model parameterized with Equations (7–9) will be adopted here as a reference, also due to its great acceptability. An inconvenience of this reference model is that with Equation (9), $K_r(h = 0) = K_{ro} \leq 1.0$, that is, generally $K(h = 0) \neq K_s$, which is an inconsistency. In spite of this, another argument for the use of Equations (7–9) in this study as a reference is that certain soils can present a dual permeability field close to saturation (suction range from zero to a few centimeters): the first permeability field takes up a greater soil volume, is relatively macroscopically homogeneous and has a slower flow, usually called matrix flow; and the second, of smaller volume than the first one, is much more heterogeneous within the soil volume and has a faster flow, called macropore or fast flow. The latter field, formed by large and clearly individualized pores or cracks, and/or large spaces between soil peds, is well described in the literature (Beven and Germann, 1982; Jarvis, 2007; Lassabatere et al., 2014; Perret et al., 1999) and its hydraulic behavior has been modeled (Jarvis, 2008; Larsbo and Jarvis, 2006; Lassabatere et al., 2014). In porous structures where this double permeability close to saturation clearly occurs, the macropore flow is commonly a major component of the total flow. As a result, the saturated and unsaturated hydraulic conductivity (in the very wet range) can be strongly influenced by the macropore flow. Outside the narrow suction range where both flows occur interactively, the macropore flow becomes null and the unsaturated hydraulic conductivity is determined by only the matrix flow. Due to the narrow suction range (approximately 0–10 cm, as proposed by Jarvis, 2007) where the macropore flows occur, various authors (Schaap and van Genuchten, 2006; van Genuchten and Nielsen, 1985; Vereecken et al., 2010) admit that the strictly empirical equations and the usual models of representation of $K_r(h)$, such as Equations (7–9), can represent only the matrix flows. For this reason, Equation (9) is used here as a reference in the representation of the $K_r(h)$ curve, despite the fact that K_{ro} in Equation (9) can be smaller than 1 (sometimes by various orders of magnitude) in soils that present macropore flow. Schaap and Leij (2000) determined an approximate mean value of $K_{ro} = 0.1$ for their database, which indicates that soils with macropore flow were frequent. In the MVG parametrization of the soil in Figure 1, $K_{ro} = 0.81$ and there is no marked tendency to dual permeability, since the data plot in the very wet range (0–10 cm suction) clearly tended to the origin of the axes smoothly and asymptotically to the log h-axes. We can see that the MVG model (Equations (7–9)) represented the data for this soil relatively well across the whole suction range.

Schaap and van Genuchten (2006) introduced a modification suggested by Vogel et al. (2001) into the MVG model (Equations (7–9)) in an attempt to improve its efficiency, mainly in the suction range close to saturation. Additionally, they also included the macropore flow effects. The final product, the modified MVG model (MVGm), was tested with the same previously mentioned database (Schaap and Leij, 2000). The representation of the $K_r(h)$ curve improved significantly (37%) in relation to Equations (7–9) (error of 0.41 in contrast to 0.26 with the MVGm model). Although this result is promising, the MVGm model has not been widely used.

Assuming that the Gardner exponential model (Equation (2)) can be satisfactorily applied in a limited suction range close to saturation, the main objective of this study was to modify this model to extend it to suction values greater than a certain transition suction value, h_o. The extended model has been labeled Gardner dual model (GD). Another objective was to describe the GD model behavior and its parameters. The proposed model will be tested with practically the same database as that used by Schaap and Leij (2000) and its performance will be compared mainly to that of the Mualem-van Genuchten (MVG) model (Equations (7–9)), but also to that of the modified MVG model (MVGm). The measured suction of the samples varied from minimum values from 1 cm to 40 cm to maximum that rarely exceeded 15000 cm.

MODEL DEVELOPMENT AND DESCRIPTION

The GD model assumes that for $h \leq h_o$, the transition suction, the depletion of K_r is exponential to the increase in h, as predicted by Equation (2). The exponential depletion will be extended to $h \geq h_o$, but on the log scales of K_r and h (h expressed in cm), that is, for $h \geq h_o$:

$$\log K_r = a + b e^{-\log h/\beta} , \quad (10)$$

where $\beta > 0$, the conductive depletion coefficient (dimensionless), is a parameter of the GD model. Constants a and b will be

calculated so that $K_r(h)$ is continuous and smooth (with continuous derivative) at $h = h_o$. Making $X = \log h$, $X_o = \log h_o$, $Y = \log K_r$, $Y_o = Y(X_o) = \log K_{ro}$ (different from K_{ro} in Equation (9), despite the same notation), which from Equation (2) is:

$$Y_o = -(\log e)h_o/\lambda, \quad (11)$$

where λ is the macroscopic capillary length and e is the Neper constant, thus:

$$a = -\frac{h_o}{\lambda}(\log e + \beta); b = \frac{h_o\beta}{\lambda} e^{\log h_o/\beta}.$$

Using Equations (2) and (11) and applying the two expressions above to Equation (10), the GD model becomes:

$$Y = Y(X) = (-\log e/\lambda)h,\ 0 \le h \le h_o, \quad (12a)$$

$$Y_o - Y = \frac{h_o\beta}{\lambda}\left[1 - e^{-(X-X_o)/\beta}\right],\ h \ge h_o. \quad (12b)$$

The derivatives of Y are:

$$dY/dX = -h/\lambda,\ 0 \le h \le h_o, \quad (13a)$$

$$dY/dX = (Y_o/\log e)e^{-(X-X_o)/\beta},\ h \ge h_o. \quad (13b)$$

$$d^2Y/dX^2 = -\frac{h}{(\log e)\lambda} < 0,\ 0 \le h < h_o, \quad (14a)$$

$$d^2Y/dX^2 = \frac{-Y_o}{(\log e)\beta} e^{-(X-X_o)/\beta} > 0,\ h > h_o. \quad (14b)$$

Analyzing the behavior of the $Y(X)$ curve at X_o, Equations (11) to (13) confirm that it is continuous and smooth, with:

$$dY/dX\left(X \to X_{o-}\right) = -h_o/\lambda = dY/dX\left(X \to X_{o+}\right) = Y_o/\log e. \quad (15)$$

X_o is a point of inflection of the $Y(X)$ curve, since Equation (14) indicates that the signal of d^2Y/dX^2 changes at X_o (and also d^2Y/dX^2 is discontinuous), and the $Y(X)$ curvature changes from convex ($d^2Y/dX^2 < 0$, $h < h_o$) to concave ($d^2Y/dX^2 > 0$, $h > h_o$), as shown in Figure 2. Equations (14b) and (15) also show that:

$$\beta = -\frac{dY/dX(X_o)}{d^2Y/dX^2(X \to X_{o+})}, \quad (16)$$

which confirms that the three model parameters (h_o, λ, β) are entirely determined by the $Y(X)$ curve behavior at the $X = X_o$ inflection point.

Using the GD model, we next define a soil structural index related to the $Y(X)$ curve, similar to the S structural index in Dexter (2004) related the water retention curve, $w(\log h)$ (w is the gravimetric water content), defined as $S = -dw/d(\ln h)$ ($h = h_o$), where h_o is the $w(\log h)$ curve inflection point and ln is the natural logarithm. This new parameter will be labeled conductive depletion index (dimensionless) and represented as the S_k index, defined as:

$$S_k = -dY/d(\ln h)\ (h = h_o). \quad (17)$$

As $dY/d(\ln h) = dY/dX \log e$, by Equations (15), (17) and (11):

$$S_k = -Y_o = -\log K_{ro} = (\log e)h_o/\lambda. \quad (18)$$

Figure 2 shows an example of fit of the $Y(X)$ curve based on the GD model; the (X_o, Y_o) inflection point and its tangent straight line are indicated, including the graphic representation of the derivative, which, according to Equations (15) and (18), is:

$$|dY/dX(X_o)| = T = \mathrm{tg}(\gamma) = S_k/\log e. \quad (19)$$

The dual model (Equation (12)) can also be calculated from Equation (20) using variable $g = h/h_o$ and the S_k index (Equation (18)):

$$-Y(g) = \log(K_r^{-1}) = S_k\, d_\beta(g), \quad (20a)$$

$$d_\beta(g) = g,\ 0 \le g \le 1, \quad (20b)$$

$$d_\beta(g) = 1 + (\beta/\log e)\left[1 - g^{-(\log e/\beta)}\right],\ g \ge 1. \quad (20c)$$

Function $d_\beta(g)$ varies as a power function, is smooth at $g = 1$ and depends only on parameter β. Its curve in Figure 3 (g is in log scale and d_β is in decimal scale) has the same shape (inverted) as that of $Y(X)$ (Figure 2), since $\log g = X - X_o$, and, from Equations (18) and (20a):

$$d_\beta = Y/Y_o = \log K_r/\log K_{ro}. \quad (21)$$

Due to Equation (21), $d_\beta(g)$ can be considered a normalized relative hydraulic conductivity curve. Thus, from Equation (20a), the parameter S_k is a multiplicative structural index of unsaturated hydraulic conductivity and the hydraulic conductivity, K_o, corresponding to Y_o:

$$K_o = K(h = h_o) = K_{ref} = K_s/(10^{Sk}), \quad (22)$$

can be considered a reference unsaturated hydraulic conductivity or a soil physical quality parameter.

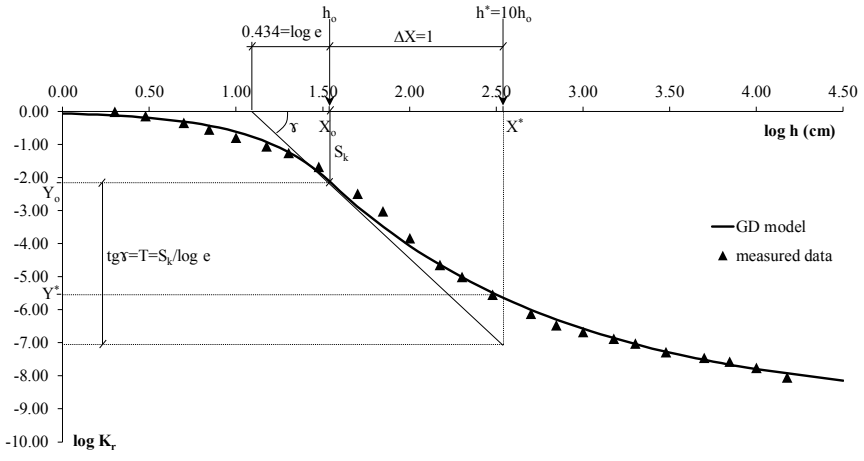

Fig. 2. Example (UNSODA database soil 4661) of fit of the experimental data to the $Y(X)$ curve calculated with the GD model; curve inflection point at h_o = 35 cm indicated. S_k index = 2.14 and the absolute value of the derivative [tg(γ)] at the curve inflection are also indicated. From Equation (18), λ = 7.09 cm. From Equation (16), the curvature of the concave part of the curve ($X > X_o$) close to its inflection depends on parameter β = 1.38.

In order to characterize the influence of parameter β on the shape of $d_\beta(g)$ curves, we defined the positive fraction F_g based on a given $g>1$ ($h> h_o$) value:

$$F_g = |(Y - Y_o)|/ [T (X - X_o)] = (Y - Y_o)/ [-T (X - X_o)], \quad (23)$$

where T is the same as in Equation (19). From Equations (18), (20a) and (20c):

$$F_g = F_g(\beta) = (\beta/\log g)(1 - g^{-\log e/\beta}) = (\beta/\log g)(1 - e^{-\log g/\beta}) \quad (24)$$

From the equation above, $\lim_{\beta \to 0} F_g = 0$, from which Equation (23) shows that Y tends to Y_o when β tends to 0, which, according to Equation (21), implies that $d_o(g) = 1$, as in Figure 3 ($g>1$). When β tends to infinite, according to Equation (14b), d^2Y/dX^2 tends to 0 and the $Y(X)$ curve tends to the straight line below:

$$Y - Y_o = -T (X - X_o), (X > X_o, \beta \to \infty). \quad (25)$$

Applying Equation (25) to Equation (23), $\lim_{\beta \to \infty} F_g = 1$ and, from Equations (18), (19), (20a) and (25):

$$d_\infty(g) = 1 + (\log g/\log e), \quad (26)$$

the same as in Figure 3, where $d_\infty(g)$ is linear ($g > 1$). Equation (25) implies that the Wind equation (Equation (1)) is a particular case of the GD model, when $h > h_o$ and β tends to infinite (or $\beta > 100$, as shown in Figure 3). In this case, power b in the Wind model is the value of $T = S_k/\log e$.

When β does not tend to zero or infinite, its influence on the shape of the $d_\beta(g)$ curves, $g > 1$, [or on the shape of $Y(X)$, $X > X_o$], is better characterized considering the particular case of fraction F_g (Equation (24)) when $g = 10$, that is:

$$F_{10} = f(\beta) = \beta [1 - e^{-(1/\beta)}]. \quad (27)$$

The $f(\beta)$ value, labeled linearization fraction, is a much more adequate parameter to describe the shape of the $Y(X)$ curve, for $X > X_o$, than parameter β. The values of $f(\beta)$ [$0 < f(\beta) < 1$] are shown in Figure 4. For $f(\beta) > 0.90$ ($\beta > 5$ approximately), Figure 3 indicates that $Y(X)$ is nearly linear; for $\beta > 100$ [$f(\beta) > 0.995$], $Y(X)$ is practically linear and invariant for β. When $f(\beta) < 0.90$ ($\beta < 5$ approximately), the linearity of $Y(X)$, $X > X_o$, can be questioned, and its curvature at X_o increases with the decrease in β, as shown in Figure 3. Therefore, the GD model flexibilizes the convex-linear shape (described in the Introduction) of the $Y(X)$ curves generated by the Gardner power and Mualem-van Genuchten models for the entire suction range, from saturation to $h > h_o$.

When the coordinates (X_o, Y_o) of the inflection point of $Y(X)$ are known, parameter β can be estimated from a single measurement of the hydraulic conductivity at a suction greater than h_o, that is, for a known value (X^*,Y^*) of pair (X,Y), $X^*>X_o$. In this case, fraction F_{g^*} can be calculated (Equations (18), (19) and (23)), and, as function $F_g(\beta)$ is invertible for any $g>1$ (since $dF_g/d\beta > 0$):

$$\beta = F_{g^*}^{-1}[F_{g^*}(\beta)] = F_{g^*}^{-1}\left[(\log e/Y_o)(Y^* - Y_o)/(X^* - X_o)\right]. \quad (28)$$

Applying the equation above to the example in Figure 2, where $X_o = \log 35$, $X^* = \log 350$, $Y_o = -2.14$, $Y_o^* \approx -5.7$ (graphically), then $g^* = 10$, $F_{g^*} = f(\beta)$, and $\beta = f^{-1}(F_{g^*} = 0.72) = 1.4$ (Figure 4).

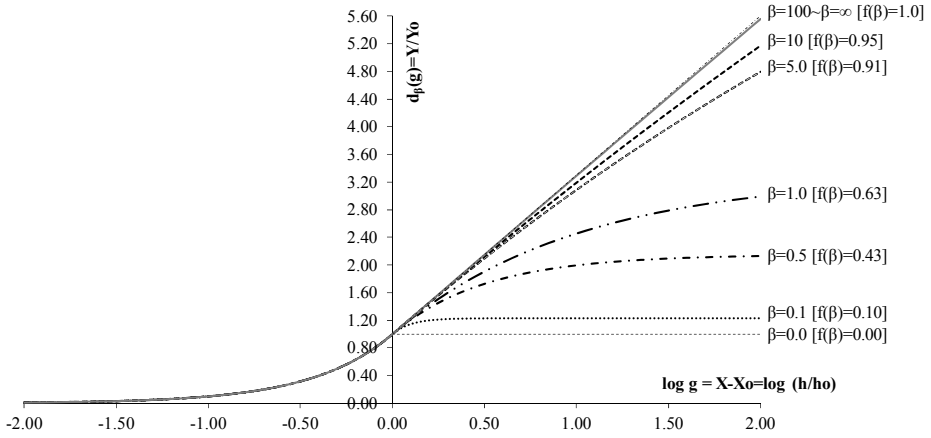

Fig. 3. Normalized relative hydraulic conductivity curve (d_β function) and its variations with parameter β, including the two limiting curves with β tending to zero and infinite. The infinite-β curve practically coincides with that of $\beta = 100$.

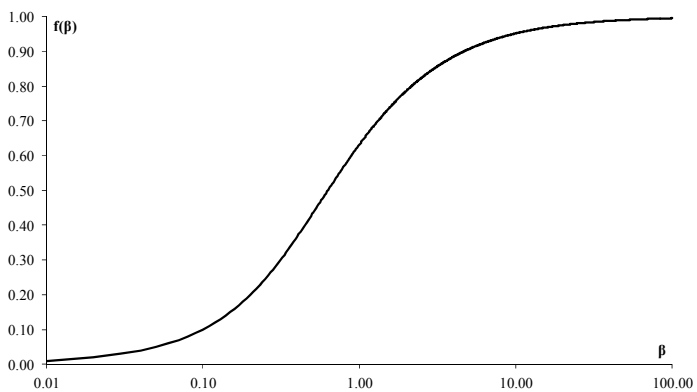

Fig. 4. Relationship between the linearization fraction, $f(\beta)$, and the conductive depletion coefficient, β.

SOIL DATABASE

Hydraulic and textural data were taken from the database in Schaap and Leij (2000), who selected 235 soil samples from the UNSODA international database (Leij et al, 1996; Nemes et al., 2001). The water retention curve data [with at least six pairs (θ, h)] and hydraulic conductivity data [with at least five pairs (K,h)] for the 235 samples were determined, as well as the saturated hydraulic conductivity values, K_s. Other information from this database, including the methods of determination of the variables, the specification and definition of the textural classes, as well the sample distribution per textural class groups, are described by Leij et al. (1996), Schaap and Leij (2000), and Nemes et al. (2001). From the 235 samples, 82 were excluded for introducing uncertainty in the optimization of the parameters of the model proposed. The most frequent source of uncertainty was the indirect determination of K_s using pedotransfer functions for 60 samples. For the other samples, K_s was determined by direct measurement. Another 17 samples were excluded because their K was measured only in a limited suction range, either under 100 cm or over 40 cm. Five more samples were omitted due to inconsistent (K, h) pair measurement close to saturation. Therefore, the database of this study contained 153 samples. The measured suction with any tested soil varied from a minimum from 1 cm to 40 cm to a maximum that rarely exceeded 15000 cm.

PARAMETER OPTIMIZATION

Let be a set of N ($N \geq 3$) data pairs of the relative hydraulic conductivity data of a sample, forming two sequences: $\{h_i,\ h_i \geq 1\ \text{cm}\}$ (increasing sequence) and $\{Y_{mi} = \log K_{rm}(h_i)\}$, $i = 1,..., N$, where subscript m indicates the measured value. The minimum limits of $h_1 = 1$ cm and $N = 3$ are arbitrary. Let $h_{\min}$ be the smallest suction value h_i such that $K_{rm}(h_i) < 1$ ($Y_{mi} < 0$) and let $h_{\max} = h_N$. For lack of data, the optimization algorithm will not work if $h_{\max} \leq 100$ cm and $h_{\min} > 40$ cm. The latter restriction results from the fact that the transition suction, h_o, cannot be optimized if $h_o < h_{\min}$ (because in this case there would not be any data to characterize the K_r depletion of Equation (2)). Therefore, so as not to jeopardize the optimization of the GD model parameters, an appropriate number of measurements at low suction range ($h_i < h_o$) is desirable. If the optimized h_o is equal to $h_{\max}$, the algorithm considers the GD model to be the Gardner exponential model.

Using Equation (12) to represent the GD model, the objective function to optimize its three parameters (h_o, λ, β) was to minimize the sum of the square errors (SSE):

$$\text{SSE} = \sum_{i=1}^{N} (Y(h_i) - Y_{mi})^2 \tag{29}$$

A Visual Basic computer program was written to interface with Microsoft Excel spreadsheets for the calculation of the algorithm of determination of the three parameters. Additionally, the program also calculates the error evaluation statistics described next. The suction and hydraulic conductivity data are inputted in the main window of the program, which also contains the routine execution buttons. The program is available from the corresponding author upon request. The alternative model parameters, S_k and $f(\beta)$, are calculated from h_o, λ and β with Equations (18) and (27), respectively.

MODEL EVALUATION

The model was evaluated based on the two indicators described below which were calculated for each soil sample: Root Mean Square Error (RMSE) and Mean Error (ME_j) for each j suction interval.

RMSE (dimensionless) is a measure of the global mean error of fitting to N pairs of sample data [(h_i, Y_{mi})], given by:

$$\text{RMSE} = \sqrt{\text{SSE}/(N-2)}\ , \tag{30}$$

where SSE is given by Equation (29) and Y by Equation (12) for the optimized model parameters. Although the GD model has three parameters, it has only two degrees of freedom as Equation (12) is defined by parts ($h < h_o$ and $h > h_o$), each part containing only one parameter (λ or β, respectively), which makes the denominator of Equation (30) equal to $(N-2)$, instead of $(N-3)$.

ME (dimensionless) complements the RMSE measure by calculating the fitting error in each of the following nine suction intervals, represented by the limits: 1.0, 3.2, 10, 32, 100, 320, 1000, 3200, 10000, 32000 cm. The value of ME_j for each j value ($1 \leq j \leq 9$) is given by:

$$ME_j = \frac{1}{N_j} \sum_{i=1}^{N_j} \left[Y(h_{ji}) - \log K_{rm}(h_{ji}) \right], \tag{31}$$

where N_j is the total number of measurement pairs [h_{ji}, $K_{rm}(h_{ji})$] in suction interval j and Y is calculated with Equation (12) using the optimized parameters. Thus, a positive or negative ME_j value indicates that the model respectively either overestimates or underestimates the K_r values in interval j.

For a sample set, the goodness of fit of the model is given by the arithmetic mean of the RMSE values of the samples, and for each j value, $j = 1,\ldots,9$, by the weighted mean of the ME_j values of the samples (with the weight equal to the number of measurements of the respective sample within interval j).

Comparison with the Mualem-van Genuchten models

The method of evaluation described above is identical to that used by Schaap and van Genuchten (2006) to evaluate the fitting errors of models MVG and MVGm, with, roughly speaking, the same database used in our study (in fact they used the 235 samples from the UNSODA database, as already mentioned, rather than the 153 samples of this study). Both models also have two degrees of freedom. All this makes the comparison of the Gardner dual model to these two models easier. The authors also kindly granted us access to their full database (personal communication). We will use the same four soil sets that they used to compare the performance of the models according to textural class groups, namely Sands, Loams, Silts and Clays.

Table 1 and Figure 5 show, respectively, the RMSE mean values and the probability distributions of the RMSE values, for models GD, MVG and MVGm. Considering the complete database (Figure 5a), we observe that model GD in general calculates the K_r curve data with intermediate accuracy in relation to the two other models, with a mean RMSE of 0.378 for GD, and 0.468 and 0.280 for the MVG and MVGm models, respectively. The goodness of fit of the GD model improves substantially when only the model's 77 best fitting soils (50% percentile) are considered, giving an RMSE < 0.32 (Figure 5a). These soils make up database A in Table 1. In this case, according to Table 1, the GD model mean error was confirmed to be 64% smaller than that of the MVG model (0.191 in contrast to

Table 1. RMSE values for the complete database and for four subsets of its soils taking into account models GD, MVG and MVGm.

Database	Number of Soils	Mean RMSE		
		GD model	MVG model	MVGm model
Complete	153	0.378	0.468	0.280
* A	77	0.191	0.525	0.269
** B	76	0.569	0.410	0.291
*** A'	55	0.236	0.558	0.278
**** B'	50	0.554	0.386	0.250

* soils with $RMSE_{GD} < 0.32$; ** soils with $RMSE_{GD} \geq 0.32$; *** soils with K_r measurements in range $h \leq 10$ cm; all K_r values > 0.10 in this suction range; **** soils with K_r measurements in range $h \leq 10$ cm; at least one K_r value ≤ 0.10 in this suction range.

0.525) and 29% smaller than that of the MVGm model (0.191 in contrast to 0.269), which indicates the superiority of the model proposed regarding the goodness of fit for A, as also shown in Figure 5b.

However, the goodness of fit of the GD model was much poorer when only soils in database B (76 soils) were considered; database B complements database A in relation to the complete database, that is, it comprises samples with $RMSE_{GD} \geq 0.32$. According to Table 1, the $RMSE_{GD}$ in this group of soils increased to 0.569, a value significantly higher than the corresponding MVG and MVGm errors (0.410 and 0.291). The differences between the $K_r(h)$ experimental data plots of databases A and B reveal that the data plots of A (Figure 6, soils 4650 and 4673 from UNSODA) tend to converge to the origin of the Cartesian axes [$K_r(h = 1) = 1$] asymptotically to the log h-axes, while those of B (Figure 7, soils 4092 and 4111) clearly do not. These four soils are common and consistent examples of the differences mentioned between the log-log graphs of the $K_r(h)$ data of databases A and B. The GD model requires that the Gardner exponential model be valid close to saturation, which it is not consistent with the plot of the experimental pairs (log h, log K_r) of B close to saturation. This has a significant negative impact on the fitting of GD for these soils. For MVG, this impact is weakened by its multiplicative parameter, K_{ro} (Equation (9)), which generally induces a better fitting of the MVG curves to the database B data in relation to the GD fitting, as shown in Figure 7. What can justify the abrupt variation of hydraulic conductivity close to saturation in soils from database B is the macropore flow phenomenon, which applies, as we have seen, only to a very limited suction range, in the order of 0–10 cm. Another reason might be experimental inconsistencies involving saturated and unsaturated hydraulic conductivity measurements very close to saturation. However, our analysis does not require the characterization of the cause of this distinct behavior of $K_r(h)$ close to saturation. For this reason, and to simplify the text, from this point on we assume that the abrupt depletion of conductivity close to K_s is due only to macropore flow.

To better support the interpretation that the main cause of the poorer goodness of fit of the GD model is the abrupt variation of the $K_r(h)$ curve measures close to saturation, we excluded the soils without K_r measures in the range $h \leq 10$ cm (48 samples) from the complete database. Two subsets were taken from the remaining database (105 samples): subset A' (55 samples), with K_r data greater than 0.10 (K "close" to K_s) in the range $h \leq 10$ cm, and subset B' (50 samples), the complement of A' in relation to the 105 soils. In this way, subset A' has only samples that did not present a marked tendency of abrupt depletion of K_r data close to saturation, while subset B' may have this tendency. A more objective criterion is thus established than that used in the previous paragraph to justify the worse performance of the GD model with database B. In fact, we observed that 85% of the samples in A' and B' belong to databases A and B, respectively. That is, the goodness of fit of the GD model was adequate (RMSE < 0.32) for most of the samples where the $K_r(h)$ data plot seems to converge asymptotically to the saturation data (Figure 5c). When the asymptotic convergence is dubious (case of B'), the GD model was normally not accurate (RMSE ≥ 0.32). Soil 4070 (Figure 8) was an exception, as the convergence was asymptotic and the GD model was not accurate (RMSE = 0.520). This sample was a peculiar case in the database, with an indication of only existing matrix flow in the whole suction range (without relevant macropore flow) and the proposed model did not fit its data accurately. The other sample in Figure 8 (soil 4670, the soil in Figure 1) is a more common example of A', which also had an indication of only matrix flow and the GD model was accurate (RMSE = 0.103). Table 1 compares the RMSE values of A' and B' for models GD, MVG and MVGm.

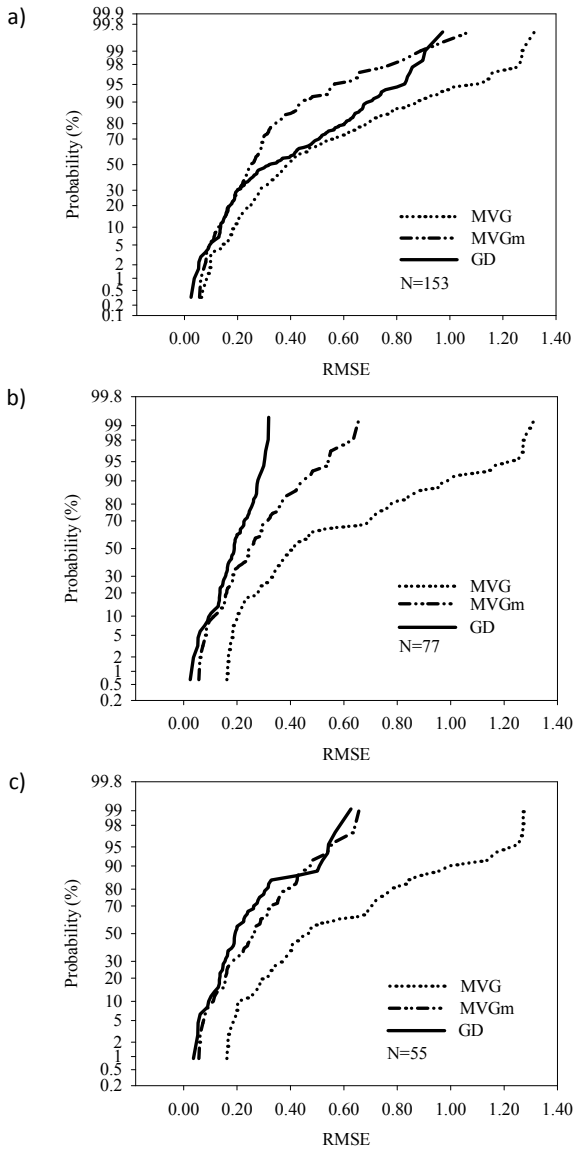

Fig. 5. Probability distribution of the RMSE values of the samples taking into account models GD, MVG and MVGm. (a) Complete soil database; (b) Soil database A ($RMSE_{GD} < 0.32$); (c) Soil database A' (soils with K_r measures in range $h \leq 10$ cm, with all K_r measures greater than 0.10 in this range).

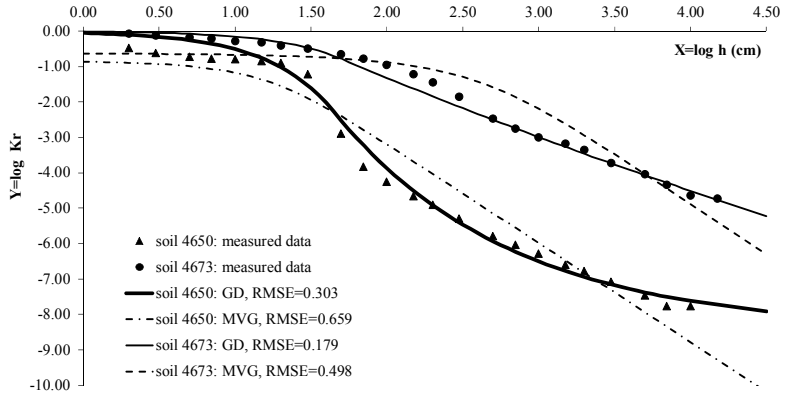

Fig. 6. Experimental data of the K_r curve and GD and MVG fits for two soils from database A, where the GD model has a good quality of fit (RMSE < 0.32).

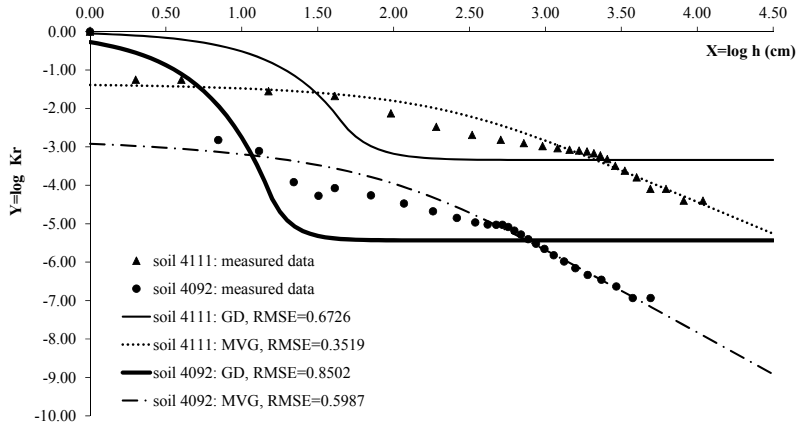

Fig. 7. Experimental data of the K_r curve and GD and MVG fits for two soils from database B, where in general the GD model does not have a good quality of fit (RMSE ≥ 0.32).

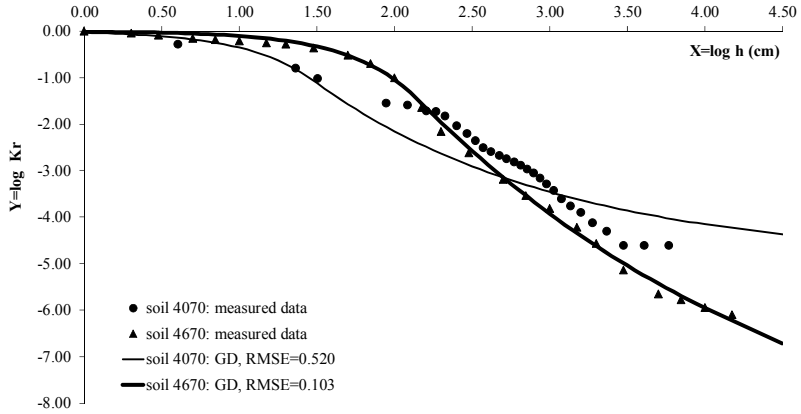

Fig. 8. Two examples of fitting of the GD model for database A', for which only matrix flow is expected to occur over the entire suction range. Soil 4670 is the most common example of GD model fitting when macropore flow is not relevant, for which GD performed well. Soil 4070 is an exception in database A', as the GD model was not efficient.

Figure 9 shows the probability distributions of the reciprocal of parameter K_{ro} of model MVG (Equation 9) for the complete database and for the 15 soils (10% of the complete database) with the worst performance for GD or MVG. In general, the more parameter $1/K_{ro}$ is different from 1, the greater the tendency of macropore flow. Figure 9 confirms the tendency of the soils with the worst performance with the GD model to have macropore flow, which does not happen in the soils with the worst performance for MVG, for which $K_{ro} = 1$ predominates. In this last case, 11 of the 15 soils are from database A ($RMSE_{GD} < 0.32$), that is, they present only matrix flow in the whole suction range, without signs of relevant macropore flow. This indicates a difficulty for the model MVG to represent hydraulic conductivity data in the matrix flow condition, which has already been shown in the literature (Schaap and Leij, 2000; Schaap and van Genuchten, 2006; van Genuchten and Nielsen, 1985; Vogel et al., 2001), and, in fact led to the development of model MVGm. Also, because MVG imposes a linear representation to the log K_r vs. log h graph at great suction ranges, in contrast to the GD model, the MVG model is unable to give a good fitting for soils that have a curved log K_r vs. log h data plot at those suction ranges. This is the case of soils 4650 (Figure 6) and 4661 (Figure 2), with $RMSE_{MVG}$ values of 0.659 and 0.581, respectively, in contrast to the corresponding $RMSE_{GD}$ values of 0.303 and 0.164. In agreement, Table 2 confirms the best performance of the GD model in comparison to the MVG and MVGm models with all textural class groups when there is only the matrix flow (with an insignificant exception for Loams). The performance of the GD model with the full database was intermediate to those of the two other models with all groups.

Figure 10 shows the calculations of the ME errors for models GD and MVG in the nine suction intervals mentioned in the beginning of this section, considering the complete database of

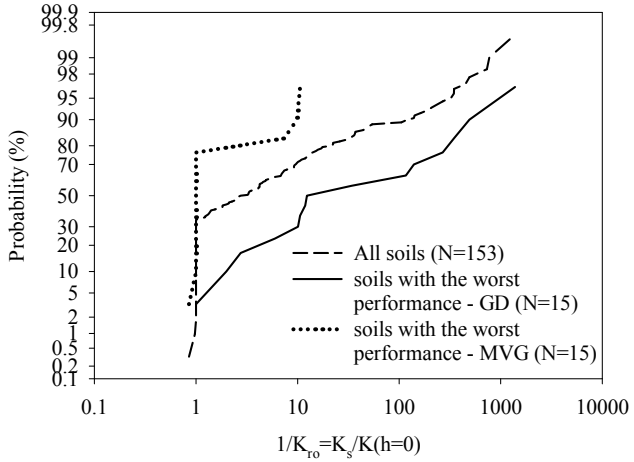

Fig. 9. Probability distribution of parameter $1/K_{ro}$ of model MVG (Equation (9)) for the complete database and the 15 soils with the worst performance with models GD and MVG.

Table 2. RMSE values per textural class for the complete database and the database of the soils that only presented matrix flow in the whole suction range (without relevant macropore flow).

	Summarized classes	Number of Soils	Mean RMSE		
			GD model	MVG model	MVGm model
Complete Database	Sands	68	0.360	0.473	0.321
	Loams	27	0.373	0.497	0.225
	Silts	40	0.431	0.444	0.263
	Clays	18	0.338	0.459	0.244
	All	153	0.378	0.468	0.280
Database A ($RMSE_{GD} < 0.32$)	Sands	37	0.203	0.465	0.286
	Loams	15	0.179	0.599	0.171
	Silts	15	0.187	0.498	0.316
	Clays	10	0.167	0.679	0.281
	All	77	0.191	0.525	0.269

our study (model GD) or that of Schaap and van Genuchten (2006) (model MVG), both with approximately the same number of samples (153 and 235 samples, as described previously). We can see that the GD errors were generally smaller or greater (in absolute value) than the MVG errors in suction intervals 1–32 cm and 32–15000 cm, respectively. When only soils without relevant macropore flow were considered (database A), the ME errors of GD were nearly null, that is, the model proposed determined the $K_r(h)$ curve without a marked bias over the whole suction range.

Evaluation of the model constants

In this subsection we considered the parameters and indexes previously described concerning the model GD in relation to the 77 soils in database A ($RMSE_{GD} < 0.32$), as these constants for database B ($RMSE_{GD} \geq 0.32$) usually refer to a poor model optimization quality and, therefore, have an inaccurate meaning. We will describe and comment how these parameters and indexes vary in A and in the four textural class groups of A (Table 3 and Figure 11, respectively). We acknowledge that this is a preliminary statistical analysis due to the reduced number of samples. Table 3 presents the soil constants in increasing order of their coefficients of variation (CV). Coefficient β was not included in Figure 11 for lack of interest for analysis.

Table 3 indicates that there are four levels of variability of soil constants in A: $f(\beta)$ and S_k (CV ≅ 37%), h_o and λ (CV ≅ 115%), K_s and K_o (CV ≅ 235%), β (CV = 319%). As already mentioned, parameter $f(\beta)$ describes the shape of the $h > h_o$ branch of the $K_r(h)$ curve better than parameter β does. The fact that β is more variable than $f(\beta)$ by approximately one order of magnitude (according to Figure 4, this occurs mainly because $f(\beta)$ is little sensitive to variations of β when $f(\beta)$ tends to 1) is another advantage to use $f(\beta)$ rather than β as a curve shape parameter. We can see in Figure 11a that the mean linearization fractions varied little in the four textural class groups, around 0.67, which indicates a little dependence of $f(\beta)$ from the soil granulometry. The $f(\beta)$ maxima tended to 1, in agreement with the situations for which the Wind model ($h > h_o$) was particularized. Very small $f(\beta)$ [$f(\beta) < 0.3$] values generally corresponded to samples with K_r measures in a very limited suction range.

Table 3. Means and coefficients of variation of the GD model soil constants for database A (77 soils), where: $f(\beta)$ is the linearization fraction, S_k - conductive depletion index, h_o - transition suction, λ - macroscopic capillary length, K_s - saturated hydraulic conductivity, K_o - reference unsaturated hydraulic conductivity, and β - conductive depletion coefficient.

	$f(\beta)$	S_k	h_o (cm)	λ (cm)	K_s (cm/d)	K_o (cm/d)	β
mean	0.672	1.59	52.8	14.5	184	6.20	20.9
CV (%)	36.1	37.8	113	116	225	243	319

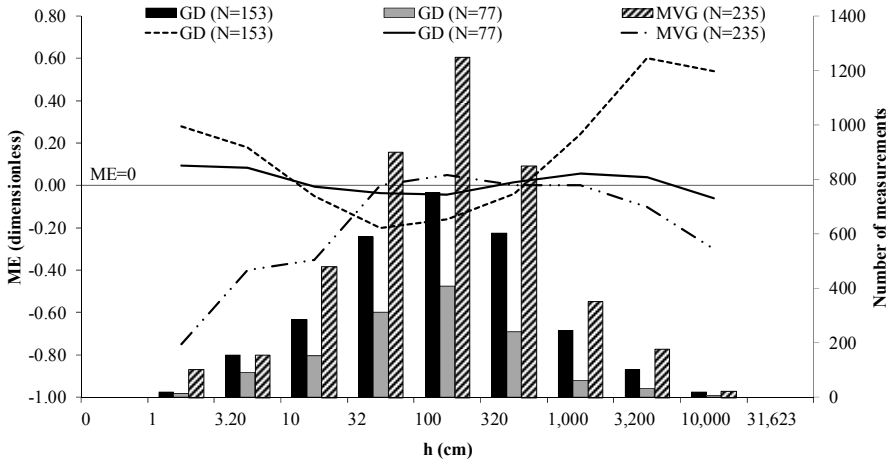

Fig. 10. Mean errors (ME) of models GD and MVG in the nine suction intervals considered (lines) and number of measurements (bars) in each interval. For MVG, we considered the Schaap and van Genuchten (2006) database, with 235 soils (results taken from the authors' Figure 4). For GD, we considered the complete database of our study (153 soils), as well as database A (77 soils) with only the soils without signs of relevant macropore flow.

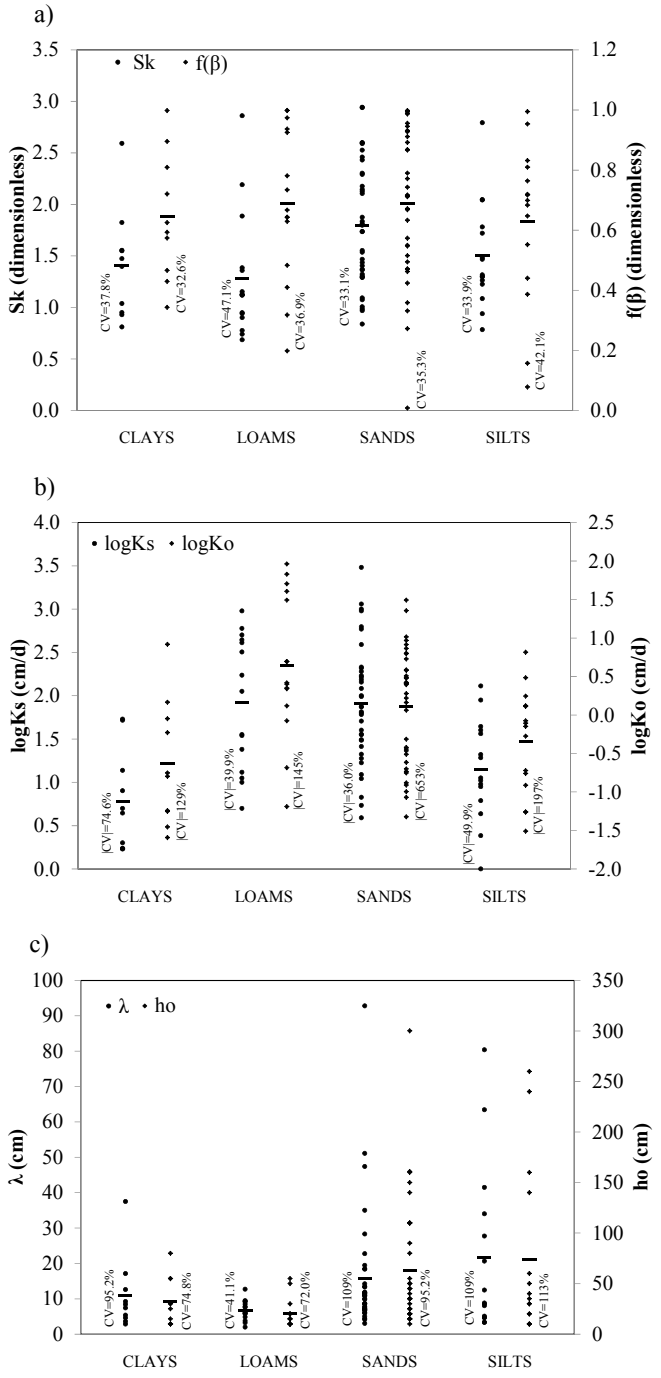

Fig. 11. Means, coefficients of variation (CV) and values of the GD model soil constants for the four textural class groups in database A: Clays - 10 soils, Loams -15 soils, Sands -37 soils, Silts - 15 soils. (a) $f(\beta)$, S_k; (b) log K_s (cm/d), log K_o (cm/d) (means and CVs of the logarithmic values); (c) h_o (cm), λ (cm).

Soils 4650 and 4673 in Figure 6 are examples of mean and high values, [$f(\beta)$ = 0.67] and [$f(\beta)$ = 0.95], respectively, of the linearization fraction, which indicates that the situation of the curvilinear shape of the $Y(X)$ (for $h > h_o$) curve of the first soil is frequent in database A. Examples of more extreme situations of the parameter are shown in Figure 12: soil 2561 [$f(\beta)$ = 0.996] and soil 2743 [$f(\beta)$ = 0.48]. Soils 4673 (Figure 6) and 2561 (Figure 12) illustrate the quasi-linear and linear branches $h > h_o$ of $Y(X)$, respectively.

The S_k index is the GD model constant better related to the global depletion capacity of the hydraulic conductivity curve, as it is a multiplicative value of $Y = \log K_r$ in the entire suction range, according to Equation (20). Another constant directly related to the depletion potential of the $K_r(h)$ curve is $f(\beta)$, but concerning only its $h > h_o$ branch. That is, the greater the S_k and $f(\beta)$ values are, the greater the depletion capacity of $K_r(h)$. Index S_k is also proportional to the absolute value of the dY/dX slope at the $Y(X)$ inflection point (Equation (19); Figures 2 and 12), at the same time that it is the absolute value of Y at this point (Equation (18); Figures 2 and 12), thus being a soil structural hydraulic parameter. As seen, another parameter with this nature is the macroscopic capillary length, λ, related to S_k by Equation (18). However, λ relates only to the branch $h < h_o$ of $Y(X)$ and its use with the GD model is unnecessary when the values of S_k and h_o are known (Equation (20)). In Figure 11a, the mean value of S_k varied between the textural class groups, indicating a certain dependence from the soil granulometry: samples in the Sands group (sand, loamy sand, sandy loam, sandy clay loam) tended to present values (S_k = 1.79) greater than those of the other groups. This confirms the general notion that in unsaturated conditions (but not very close to saturation), sandy soils tend to be less permeable than the others (Hillel, 1998). S_k had the smallest mean value in the Loams (loam and clay loam) group (S_k = 1.28). The maxima and minima for the four textural class groups were approximately 2.8 and 0.75, respectively. Figure 12 presents examples of $Y(X)$ curves for low (S_k = 0.90, soil 2743), medium (S_k = 1.45, soil 4670) and high (S_k = 2.13, soil 2561) depletion index conditions. Soil 2561 is a sand with a high depletion potential for the $K_r(h)$ curve; K decreases by eight orders of magnitude between saturation and the suction value of 350 cm. In addition to S_k, its $f(\beta)$ parameter is also high [$f(\beta)$ = 0.996], which contributes to an increase in the conductive depletion. Sample 2743 is an opposite example: a clay loam with a low depletion potential. In this case, for the suction value of 160 cm, the K value decreased by only two orders of magnitude in relation to the saturation. Extrapolating the GD model to this soil at suctions greater than 160 cm, with both small S_k and $f(\beta)$ values, the conductive depletion must remain very low, as indicated in Figure 12. Soil 4670 is an intermediate example of the depletion potential of the $Y(X)$ curve in relation to the other two soils.

The reference unsaturated hydraulic conductivity, $K_o = K(h_o)$, was calculated with Equation (22). It is a soil physical quality parameter, as it depends exclusively on the saturated hydraulic conductivity (K_s) and the S_k index. In the three soil examples above, the respective K_s and K_o of 2561 (sand), 2743 (clay loam) and 4670 (silt) are (in cm/d): (3020, 23), (320, 40), (89, 3.0), which indicates a distinct level and ordination of reference unsaturated hydraulic conductivity values in relation to the saturated values. Figure 11b illustrates the distributions of the log K_s and log K_o values for the four textural class groups. The geometric mean value (4.40 cm/d) of K_o of the Loams group was approximately three times larger than the geometric mean (1.30 cm/d) of the Sands group and one order of magnitude greater than those of the other two groups. As the transition suction (h_o) normally corresponded to a wet soil situation (mean h_o = 52.8 cm, Table 3), we conclude that in the wet range (but not very close to saturation) of database A, the soils from the Loams group tend to have a greater hydraulic conductivity in comparison to the other soils.

Among the three parameters, h_o, λ and S_k, only two are needed for the calculation of $K_r(h)$, because of Equation (18). Figure 11c shows the distribution of the h_o and λ values in the four textural class groups, which shows that with only one exception (λ in the Loams group), these parameters were much more variable than the third parameter; their coefficients of variation

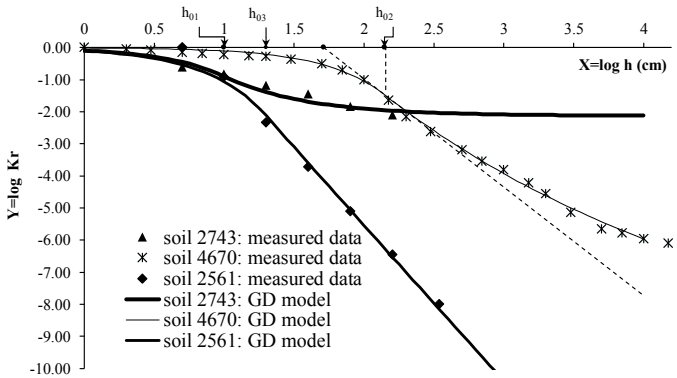

Fig. 12. Three examples of GD model fitting involving soils with low (S_{k1} = 0.90, soil 2743), mean (S_{k2} = 1.45, soil 4670) and high (S_{k3} = 2.13, soil 2561) S_k indexes from database A. The other parameters are: soil 2743 (h_{o1} = 10 cm, λ_1 = 4.8 cm, $f_1(\beta)$ = 0.48), soil 4670 (h_{o2} = 140 cm, λ_2 = 41.5 cm, $f_2(\beta)$ = 0.83), soil 2561 (h_{o3} = 20 cm, λ_3 = 4.1 cm, $f_3(\beta)$ = 0.996). The transition suction values of the three curves are indicated. The tangent at the inflection of the $Y(X)$ curve is shown only for soil 4670.

in general were at least twice as great as those of S_k. This might indicate a greater difficulty in the indirect estimation of h_o and λ using pedofunctions rather than in the estimate of S_k. The h_o and λ mean values also seem to vary with soil granulometry. They were greater in groups Sands and Silts, smaller in the other two groups and maximum in the Silts group (h_o = 74 cm, λ = 21.8 cm). The transition suction value was limited to the 10–300 cm range, showing that the experimental determination of the X_o, Y_o coordinates of the inflection point of $Y(X)$, of great relevance in the characterization of the GD model parameters, must be restricted to the wet range of the hydraulic conductivity curve (where suction can be monitored by tensiometry), which is greatly advantageous. This h_o range is consistent with the suction values at the inflection points of the (log K_r) vs (log h) curves of Figures 2 and 3 in Peters and Durner (2008). Parameter λ was within range 2.0–93 cm, with mean value of 14.5 cm, which is consistent with the literature (Communar and Friedman, 2014; Reynolds, 2016; White and Sully, 1987). This parameter is commonly considered a measure of the soil dynamic capillarity. Usually, medium and fine textured soils are considered to have greater λ values, and coarser soils, smaller values (Communar and Friedmand, 2014, Reynolds, 2016). However, in database A, Sands tended to have a greater λ than Clays and Loams (Figure 11c). Yet, White and Sully (1987) admitted that soil granulometry should not influence this parameter markedly. On the other hand, the small number of samples in database A makes a more judicious analysis difficult. It is also commonly accepted that soils with greater λ values (more "capillary") are less depletive in terms of $K_r(h)$ than those with smaller λ values. This holds only in the suction range to which the Gardner exponential model applies. In wider suction ranges, according to Equation (18), the depletion potential of $K_r(h)$ (S_k index) also depends on the value of h_o, when compared to λ. This is the case of sand 2561 in Figure 12, which is much more depletive than clay loam 2743, despite their very close λ values, what is justified by their very distinct h_o values, in a relative comparison (h_o = 20 cm and 10 cm, respectively). This is also the case of silt 4670 in Figure 12, globally more depletive than soil 2743, despite its far greater "dynamic capillarity" (λ = 41.5 cm and 4.8 cm, respectively).

CONCLUSION

The model proposed, called the Gardner dual model (GD model) is, in fact, a natural extension of the Gardner exponential model of hydraulic conductivity (Equation 2), since the extension equation (Equation 10), for $h > h_o$, expresses the same law of exponential decay of hydraulic conductivity with suction, only changing the decimal scales of h and K_r (Equation 2) by the corresponding logarithmic scales (Equation 10). The transition suction from the decimal to the logarithmic law, h_o, might result from a change of soil hydraulic behavior as the porous space becomes drier, as suggested by Peters and Durner (2008). The GD model was more accurate than the two-parameter (K_{ro} and L) Mualem-van Genuchten model (MVG model) and the corresponding modified MVG model (MVGm model) in the representation of the $K_r(h)$ curve in 77 soils that did not present relevant macropore flow. In this case, the mean RMSE of the model proposed was 64% smaller (0.191 to 0.525) and 29% smaller (0.191 to 0.269) than those of the MVG and MVGm models, respectively; the GD model also calculated $K_r(h)$ more efficiently than the MVG model in all suction ranges. The remaining 76 soils generally presented signs of relevant macropore flow, which tended to lead to poorer performance of the GD model in all suction ranges and to a generally lower accuracy than those of the other two models. We conclude that the mathematical representation of the GD model was more adequate than those of the MVG and MVGm in soils with only matrix flow in the whole suction range. On the other hand, the GD model is not recommended for soils with dual permeability close to saturation. Therefore, modifying the GD model to include the effects of macropore flow is an interesting possibility. Another issue that deserves investigation is the determination of the suction upper limit beyond which the GD model is not valid. In this paper the model was evaluated for suctions smaller than 15000 cm.

Like models MVG and MVGm, the proposed model has two degrees of freedom, although it requires three parameters for its calculations. One of the parameters is the conductive depletion coefficient, (β), or, alternatively, the linearization fraction [$f(\beta)$], which are dimensionless shape parameters of the hydraulic conductivity curve, as shown in Figure 3. The other two model parameters depend strictly on the coordinates X_o, Y_o of the inflection point of the $Y(X)$ curve, where X = log h, Y = log K_r. They are the transition suction, h_o (cm), and the conductive depletion index, S_k (dimensionless). The first is the suction at the inflection of the $Y(X)$ curve, the limit suction value of the range in which the classic Gardner exponential model is applicable. The second parameter, S_k, is the absolute value of log K_r at h_o, with the definition of S_k similar to that of the S index of the water retention curve. The macroscopic capillarity length λ (cm), a physical parameter known in the infiltration literature, can be calculated from h_o and S_k. Thus, this study has demonstrated that the determination of the GD model parameters is highly dependent on the measurement of the $Y(X)$ curve at suction values close to its inflection (see also Equation (28)), which is an experimental advantage, since the transition suction, h_o, has been demonstrated to be within a wet range (h_o = 10 to 300 cm). This must favor the estimation of the hydraulic conductivity in a wide suction range after the optimization of the GD model parameters using only the experimental data in the wet range with suction values around h_o.

REFERENCES

Beven, K., Germann, P., 1982. Macropores and water flow in soils. Water Resour. Res., 18, 1311–1325.

Campbell, G.S., 1974. A simple method for determining unsaturated conductivity from moisture retention data. Soil Sci., 17, 311–314.

Clothier, B., Scotter, D., 2002. Unsaturated water transmission parameters obtained from infiltration. In: Dane, J.H., Topp, G.C. (Eds.): Methods of Soil Analysis, Part 1. SSSA Book Ser. 4, SSSA, Madison, WI, pp. 879–889.

Communar, G., Friedman, S.P., 2014. Determination of soil hydraulic parameters with cyclic irrigation tests. Vadose Zone J., 13, 4, 12 p, DOI: 10.2136/vzj2013.09.0168.

Dexter, A.R., 2004. Soil physical quality. Part I. Theory, effects of soil texture, density, and organic matter, and effects on root growth. Geoderma, 120, 201–214.

Gardner, W.R., 1958. Some steady-state solutions of the unsaturated moisture flow equation with application to evaporation from a water table. Soil Sci., 85, 228–232.

Jarvis, N.J., 2007. A review of non-equilibrium water flow and solute transport in soil macropores: principles, controlling factors and consequences for water quality. European Journal of Soil Science, 58, 523–546.

Jarvis, N.J., 2008. Near-saturated hydraulic properties of macroporous soils. Vadose Zone J., 7, 1302–1310.

Jarvis, N.J., Messing, I., 1995. Near-saturated hydraulic conductivity in soils of contrasting texture as measured by tension infiltrometers. Soil Sci. Soc. Am. J., 59, 27–34.

Kosugi, K.I., Hopmans, J.W., Dane, J.H., 2002. Water retention and storage: Parametric models. In: Dane, J.H., Topp, G.C. (Eds.): Methods of Soil Analysis, Part 1. SSSA Book Ser. 4, Madison, WI, pp. 739–757.

Lassabatere, L., Yilmaz, D., Peyrard, X., Peyneau, P.E., Lenoir, T., Simunek, J., Angulo-Jaramillo, R., 2014. New analytical model for cumulative infiltration into dual-permeability soils. Vadose Zone J., 13, 15pp. DOI: 10.2136/vzj2013.10.0181.

Larsbo, M., Jarvis, N., 2006. Information content of measurements from tracer microlysimeter experiments designed for parameter identification in dual-permeability models. J. Hydrol., 325, 273–287.

Lazarovitch, N., Ben-Gal, A., Simunek, J., Shani, U., 2007. Uniqueness of soil hydraulic parameters determined by a combined Wooding inverse approach. Soil Sci. Soc. Am. J., 71, 860–865.

Leij, F.J., Alves, W.J., van Genuchten, M.Th, Williams, J.P., 1996. The UNSODA unsaturated soil hydraulic database, version 1.0, EPA report EPA/600/R-96/095, EPA National Risk Management Laboratory, G-72, Cincinnati, OH.

Leij, F.J., Russel, W.B., Lesch, S.M., 1997. Closed-form expressions for water retention and conductivity data. Ground Water, 35, 5, 848–858.

Mualem, Y., 1976. New model for predicting hydraulic conductivity of unsaturated porous media. Water Resour. Res., 12, 513–522.

Nemes, A., Schaap, M.G., Leij, F.J., Wosten, J.H.M., 2001. Description of the unsaturated soil hydraulic database UNSODA version 2.0, J. Hydrol., 251, 151–162.

Perret, J., Prasher, S.O., Kantzas, A., Langford, C., 1999. Three-dimensional quantification of macropore networks in undisturbed soil cores. Soil Sci. Soc. Am. J., 63, 1530–1543.

Peters, A., Durner, W., 2008. A simple model for describing hydraulic conductivity in unsaturated porous media accounting for film and capillary flow. Water Resour. Res., 44, W11417. DOI: 10.1029/2008WR007136.

Philip, J.R., 1969. Theory of infiltration. Adv. Hydrosci., 5, 215–296. DOI: 10.1016/B978-1-4831-9936-8.50010-6.

Philip, J.R., 1986. Linearized unsteady multidimensional infiltration. Water Resour. Res., 22, 1717–1727.

Poulsen, T.G., Moldrop, P., Yamaguchi, T., Jacobsen, O.H., 1999. Predicting saturated and unsaturated hydraulic conductivity in undisturbed soils from soil water characteristics. Soil Sci., 164, 877–887.

Raats, P.A.C., Gardner, W.R., 1971. Comparison of empirical relationships between pressure head and hydraulic conductivity and some observations on radially symmetric flow. Water Resour. Res., 7, 921–928.

Russo, D., 1988. Determining soil hydraulic properties by parameter estimation: On the selection of a model for the hydraulic properties. Water Resour. Res., 24, 453–459.

Reynolds, W.D., Elrick, D.E., Clothier, B.E., 1985. The constant head well permeameter: Effect of unsaturated flow. Soil Sci., 139, 172–180. DOI: 10.1097/00010694-198502000-00011.

Reynolds, W.D., Elrick, D.E., 1990. Ponded infiltration from a single ring: I. Analysis of steady flow. Soil Sci. Soc. Am. J., 54, 1233–1241.

Reynolds, W.D., 2008a. Saturated hydraulic properties: Ring infiltrometer. In: Carter M.R., Gregorich E.G. (Eds.): Soil Sampling and Methods of Analysis. 2nd ed. CRC Press, Boca Raton, FL, pp. 1043–1056.

Reynolds, W.D., 2008b. Unsaturated hydraulic properties: Field tension infiltrometer. In: Carter, M.R., Gregorich, E.G. (Eds.): Soil Sampling and Methods of Analysis. 2nd ed., CRC Press, Boca Raton, FL, pp. 1107–1127.

Reynolds, W.D., 2008c. Saturate4d hydraulic properties: Well permeameter, In: Carter, M.R., Gregorich, E.G. (Eds.): Soil Sampling and Methods of Analysis. 2nd ed., CRC Press, Boca Raton, FL, pp. 1025–1042.

Reynolds, W.D., 2011. Measuring soil hydraulic properties using a cased borehole permeameter: Falling-head analysis. Vadose Zone J., 10, 999–1015. DOI: 10.2136/vzj2010.0145.

Reynolds, W.D., 2016. A unified Perc Test-well permeameter methodology for absorption field investigations. Geoderma, 264, 160–170. http://dx.doi.org/10.1016/j.geoderma.2015.10.015

Schaap, M.G., Leij, F.J., 1998. Using neural networks to predict soil water retention and soil hydraulic conductivity. Soil & Tillage Research, 47, 37–42.

Schaap, M.G., Leij, F.J., 2000. Improved prediction of unsaturated hydraulic conductivity with the Mualem-van Genuchten model. Soil Sci. Soc. Am. J., 64, 843–851.

Schaap, M.G., van Genuchten, M.Th., 2006. A modified Mualem-van Genuchten formulation for improved description of the hydraulic conductivity near saturation. Vadose Zone J., 5, 27–34.

van Genuchten, M.Th., 1980. A closed-form equation for predicting the hydraulic conductivity in unsaturated soils. Soil Sci. Soc. Am. J., 44, 892–898.

van Genuchten, M.Th., Nielsen, D.R., 1985. On describing and predicting the hydraulic properties of unsaturated soils. Annales Geophysicae, 3, 615–628.

Vandervaere, J.-P., 2002. Unsaturated water transmission parameters obtained from infiltration: Three-dimensional infiltration using disk permeameters: Early-time observations, In: Dane, J.H., Topp G.C. (Eds.): Methods of Soil Analysis, Part 1, SSSA Book Ser. 4, Madison, WI.

Vogel, T., van Genuchten, M.Th., Cislerova, M., 2001. Effect of the shape of the soil hydraulic functions near saturation on variably-saturated flow predictions. Advances in Water Resources, 24, 133–144.

Vereecken, H.J., Maes, Feyen, J., 1990. Estimating unsaturated hydraulic conductivity from easily measured soil properties. Soil Sci., 149, 1–12.

Vereecken, H., Weynants, M., Javaux, M., Pachepsky, Y., Schaap, M.G., van Genuchten, M.Th., 2010. Using pedotransfer functions to estimate the van Genuchten-Mualem soil hydraulic properties: A review. Vadose Zone J., 9, 1–26.

Warrick, A.W., 1974. Time-dependent linearized infiltration. I. Point sources. Soil Sci. Soc. Am. Proc., 38, 383–386. DOI: 10.2136/sssaj1974.03615995003800030008x.

Weynants, M., Vereecken, H., Javaux, M., 2009. Revisiting Vereecken pedotransfer functions: Introducing a closed-form hydraulic model. Vadose Zone J., 8, 86–95. DOI: 10.2136/vzj2008.0062.

White, I., Sully, M.J., 1987. Macroscopic and microscopic capillary length and time scales from field infiltration. Water Resour. Res., 23, 1514–1522.

Wind, G.P., 1955. Field experiment concerning capillary rise of moisture in heavy clay soil. Neth. J. Agric. Sci., 3, 60–69.

Wooding, R.A., 1968. Steady infiltration from a shallow circular pond. Water Resour. Res., 4, 1259–1273.

Wösten, J.H.M., Pachepsky, Y.A., Rawls, W.J., 2001. Pedotransfer functions: Bridging the gap between available basic soil data and missing soil hydraulic characteristics. J. Hydrol., 251, 123–150.

Received 7 December 2018
Accepted 27 March 2019